Colloid Polym Sci 277:646–657 (1999)

ORIGINAL CONTRIBUTION

P. Sajkiewicz
A. Wasiak

Crystallite orientation during melting of oriented ultra-high-molecular-weight polyethylene

Received: 11 September 1998
Accepted in revised form: 18 February 1999

P. Sajkiewicz (✉) · A. Wasiak
Institute of Fundamental Technological Research, Polish Academy of Sciences
Świętokrzyska 21, 00-049 Warsaw
Poland
e-mail: psajk@ippt.gov.pl
Tel.: +48-22-8261281 ext. 148
Fax: +48-22-8269815

Abstract The changes in crystallite orientation during melting of oriented ultra-high-molecular-weight polyethylene (UHMW PE) were investigated by means of wide-angle X-ray scattering. The orientation distribution of crystallites in drawn UHMW PE is composed of two components differing in width. The narrow and broad components revealed in this study indicate the existence of two classes of crystallites with different orientability. Some of the crystallites are oriented almost perfectly even at low-draw ratios, while the others do not orient so effectively. The analysis of melting behaviour of such a texture composed of orthorhombic crystals indicates that highly oriented crystallites are formed by taut molecules and transform first to the hexagonal phase, while the molecules constituting low-oriented crystallites melt directly to the typical amorphous phase. The increase in orientation of highly oriented crystallites during their partial melting, observed in the samples kept at constant length and even those allowed to shrink under constant load, can be explained by the kinetic factor proposed by Ziabicki.

Key words Oriented polymers – Melting – Ultra-high-molecular-weight polyethylene

Introduction

When mechanical stress is applied to a polymer system, the molecules respond with deformation as well as with some changes in their orientation. The thermodynamic potential of the system is changed and there is no doubt that the significant effect in a system with long, flexible chains concerns the entropy of the molecules. It is well known from several experiments that the melting temperature of oriented polymers increases above the value for unoriented systems. The majority of early theories explained this fact by the deformation of molecules leading to a decrease in entropy in the amorphous phase. A few years ago Ziabicki [1, 2] introduced a model of crystal nucleation in oriented systems and showed that the critical temperature of transitions is orientation-dependent. Ziabicki [1, 2] argued that in the case of asymmetric molecular units the process of aggregation required consistent orientation of reacting molecular units. During crystallization only those elements can be effectively attached to the growing cluster whose disorientation with respect to the cluster, $\Delta\vartheta = |\vartheta_{cl} - \vartheta_s|$, does not exceed some "tolerance angle" (Fig. 1). The elements outside the tolerance range cannot be attached to the cluster and remain ineffective. This consistency, valid within the range of the "tolerance disorientation angle", segregates reacting molecules and clusters into separate classes of orientation. Since only a fraction H of single elements are effective in formation of a cluster oriented at the angle ϑ, the free energy of nucleation should be completed with an additional term $-kT(v/v_0 - 1)\ln H(\vartheta)$

$$\Delta F = \Delta F_e - kT(v/v_0 - 1)\ln H(\vartheta) \quad (1)$$

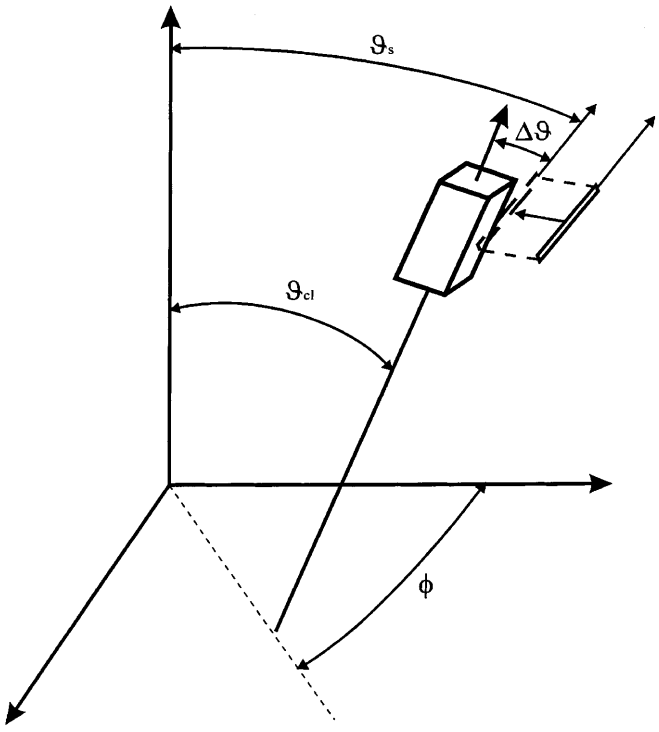

Fig. 1 Nucleation in the system of asymmetric, orientable single elements. ϑ and ϕ are orientation angles (*cl* of the cluster, *s* of single elements), $\Delta\vartheta$ is the disorientation angle of a single element with respect to the cluster

ϑ denotes the orientation of the aggregating molecular units (or cluster) with respect to the sample fixed system of coordinates, v/v_0 is the reduced volume of the cluster, ΔF_e is the free energy of the system where all single elements are equally effective in cluster formation. The additional term in the free-energy expression describes the entropy of mixing of effective and ineffective molecular units. Since the critical temperature T_{cr} of the transition is determined by the density of the free energy at the limit of infinitely large clusters ("thermodynamic" limit)

$$\lim_{v\to\infty}[\Delta F(T,\vartheta)/v] = 0 \quad \Rightarrow \quad T = T_{cr}(\vartheta) \tag{2}$$

the additional term in Eq. (1) will affect the value of T_{cr}.

The fraction H of single elements effective for addition to a cluster oriented at ϑ is defined by

$$H(\vartheta) = \int_{\vartheta-\Delta\omega/2}^{\vartheta+\Delta\omega/2} w_s(\vartheta)\,\mathrm{d}\vartheta \approx w_s(\vartheta)\,\Delta\omega \ , \tag{3}$$

where $\Delta\omega$ is the "tolerance disorientation angle" (an effective cross-section in the orientation space [3]). It is seen from Eq. (3) that in the system with nonrandom orientation distribution, $w_s(\vartheta)$, the number of single elements effective in formation of a cluster oriented at the angle ϑ depends on the orientation ϑ of the cluster with respect to the sample fixed system of coordinates. Therefore, the free energy of nucleation, ΔF, and the critical temperature, T_{cr}, appear to be differentiated with respect to cluster (crystal) orientation.

Taking a randomly oriented, unstressed system as a reference, Ziabicki has shown that in a uniaxially oriented system (single orientation angle, ϑ) the total free energy (including the elastic entropy of the deformed polymer) of the transition is described by

$$\Delta F(\vartheta) = \Delta F_0 - kT(v/v_0 - 1)\,\ln[w_s(\vartheta)/w_0] - (v/v_0 - 1)T\delta s \ , \tag{4}$$

where ΔF_0 is the free energy of the transition in a randomly oriented, unstressed system, $w_s(\vartheta)$ is the orientation distribution of crystallizing molecular units, w_0 is a constant representing the orientation distribution of such units in an unoriented system, and δs is the average elastic entropy of the deformed polymer chain. Taking into account that in the absence of orientation or stress the critical transition temperature (melting temperature) is

$$T_{m0} = \frac{\Delta h_0}{\Delta s_0} \ , \tag{5}$$

where Δh_0 and Δs_0 and the enthalpy and entropy densities in the absence of orientation, the resulting nucleation temperature is obtained in the form [1, 2]

$$\frac{T_{cr}(\vartheta)}{T_{m0}} = \frac{\Delta h_0}{\Delta h_0 + T_{m0}\{\delta s + k\ln[w_s(\vartheta)/w_0]\}} \ . \tag{6}$$

The critical nucleation temperature is a function of orientation angle, ϑ, and a functional of the orientation

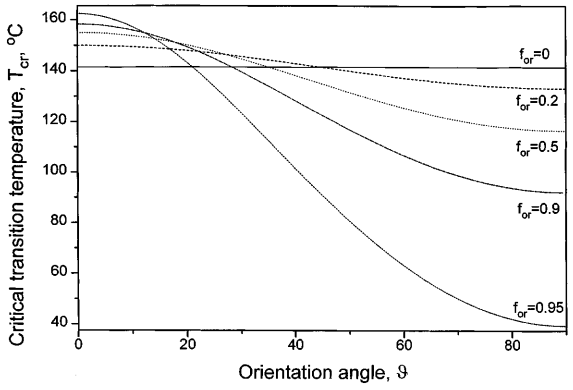

Fig. 2 Critical transition temperature, T_{cr} calculated from Eq. (6) for uniaxially oriented polyethylene as a function of orientation with respect to the draw axis, ϑ. The elastic entropy term is neglected. $T_{m0} = 414.6$ K, Segment orientation distribution $w_s = 1/4\pi \ C(A)\exp(-A\sin^2\vartheta)$, where $C(A) = \sqrt{A}/W(\sqrt{A})$ and $W(\sqrt{A}) = \exp(-A)\int_0^{\sqrt{A}}\exp(t^2)\,\mathrm{d}t$, $w_0 = 1/4\pi$. Orientation factor $f_{or} = 3/2\langle\cos^2\vartheta\rangle - 1/2 = (3[\sqrt{A} - W(\sqrt{A})]/4A\cdot W(\sqrt{A})) - \frac{1}{2}$ indicated

distribution of crystallizing molecular units, $w_s(\vartheta)$: this is shown in Fig. 2. Since the enthalpy of crystallization, Δh_0, is negative, the crystallization temperature is elevated in the range of angles where $w_s > w_0$ (near orientation axis) and is suppressed below T_{m0} for orientations perpendicular to the axis ($w_s < w_0$). The elevation (and suppression) of critical temperatures is stronger the higher the average orientation in the crystallizing system, $f_{or} = (3\langle\cos^2\vartheta\rangle - 1)/2$. In the absence of orientation ($f_{or} = 0$) the crystallization temperature is a constant ($T_{cr} = \text{constant} = T_{m0}$).

In condensed polymer systems with low mobility of clusters (crystals), T_{cr} can be identified with the apparent melting temperature, although it does not correspond to the global thermodynamic equilibrium.

The crystal orientation distribution is controlled by the orientation of crystallizing molecular units [4, 5]. According to Ziabicki, the steady-state distribution of nuclei (i.e. critical size g^* clusters which spontaneously grow to macroscopic dimensions) can be approximated by the formula [6]

$$\rho_{st}[g^*(\vartheta),\vartheta] \cong \rho_1(\vartheta)\,\exp\left(\frac{-\Delta F^*(\vartheta)}{kT}\right) = \text{const.}\; w_s(\vartheta)\,\exp\left(\frac{-\Delta F^*(\vartheta)}{kT}\right)\quad, \tag{7}$$

where ρ_1 denotes the density of orientation of single kinetic elements in the system, and ΔF^* is the critical free energy of cluster formation. It should be noted that the critical cluster distribution is a strong function of orientation, much stronger than the distribution of kinetic elements, $w_s(\vartheta)$. When the kinetics of nucleation is much faster than the reorientation of crystals due to rotational diffusion, the distribution of crystal orientation w_c is uniquely determined by the distribution of critical size clusters

$$w_c(\vartheta) \to \rho_{st}[g^*(\vartheta),\vartheta]\quad. \tag{8}$$

The dependence of the critical transition temperature on the orientation of the crystallizing units and through Eqs. (7) and (8) on the orientation of the crystals leads to some specific changes in crystallite orientation during the crystallization and melting of oriented polymers. Consider the heating of uniaxially oriented systems. In the range of temperatures $T < T_{cr}(\pi/2)$ all crystals are stable and no melting should be observed. Heating to the temperature $T_1 = T_{cr}(\vartheta_1) > T_{cr}(\pi/2)$ leads to the melting of all crystals contained in the angular interval $(\vartheta_1, \pi/2)$. Raising the temperature to $T_2 = T_{cr}(\vartheta_2) > T_{cr}(\vartheta_1)$, eliminates all crystals oriented in the interval $(\vartheta_1, \vartheta_2)$, etc. Such fractional melting is associated with the narrowing of the observed crystal orientation distribution. When the heating temperature reaches the highest level of the existence of crystals, $T_l = T_{cr}(\vartheta = 0)$, the last (ideally oriented) crystals have melted. In the case of crystallization (cooling) the transition would start with the molecules oriented parallel to the fibre axis and will continue including the segments with gradually decreasing orientation; hence, in this case the observed crystallite orientation distribution should broaden with increasing crystallinity.

There are only few experimental data dealing with the changes in crystallite orientation during phase transitions in polymers. Most of them were obtained for samples kept at constant length. Illers [7] observed a very small decrease in crystallite orientation while keeping polyethylene (PE) samples at 141 °C for 30 min at constant length. Cousin and Michel [8] have shown an increase in crystallite orientation in PVC during annealing of samples at 140 °C for 2 h. More systematic investigations showing the changes in crystallite orientation as a function of temperature (crystallinity) during crystallization at constant length were performed by Krigbaum and Maruno [9] on polystyrene, and Wasiak [10], Cesari et al. [11] as well as Hashimoto et al. [12] on crosslinked polybutadiene. In the case of polybutadiene [10–12] the crystallite orientation increased with increasing crystallization temperature. These results agree qualitatively with the data for polystyrene [9] showing a decrease in orientation with increasing crystallinity. An attempt to determine the changes in crystallite orientation as a function of crystallization temperature for crosslinked polybutadiene kept at a constant ratio of the stress to the crystallization temperature was made by Wasiak [10]. The constant ratio of the stress to the actual temperature allows the approximately constant amorphous orientation during the phase transition resulting from the dynamic equilibrium between the hydrodynamic field and rotational diffusion to be kept. This situation provides convenient conditions for the observation of the effect of the kinetic factor introduced by Ziabicki on crystallite orientation distributions during phase transitions. Wasiak [10] showed that the crystallite orientation increases slightly with crystallization temperature and this can be a qualitative argument for the existence of the kinetic mechanism predicted by Ziabicki. The fact that the degree of orientation of crystallites formed during high-speed spinning is much higher than that of the amorphous phase [13, 14] can be also interpreted as a consequence of the orientation-selective crystallization predicted by Ziabicki.

Our paper deals with investigations of the changes in crystallite orientation during partial melting occuring in deformed physical networks under various external mechanical constraints. We correlate the narrowing of the crystallite orientation distribution during partial melting with the kinetic mechanism of crystallization predicted by Ziabicki. The application of various mechanical conditions allows the intensity of the molecular reorientation caused by the hydrodynamic field to be varied. Although we did not measure the orientation of the amorphous phase, but confined our

measurements to orientations of crystals, our conditions for sample preparation and treatment ensure that the molecular orientation of the amorphous part always accompanies oriented crystals.

Experimental

Materials

Drawn foils of ultra-high-molecular-weight (UHMW) PE Hercules 1900 ($M_w = 3.7 \times 10^6$ g mol^{-1}) were investigated. Foils were formed using the gel method introduced by Smith and Lemstra [15– 18]. The procedure of sample formation was described in detail in Refs. [19, 20]. The concentration of the polymer in decaline was 0.5 wt%, slightly exceeding the value necessary to form the coherent gel. Foils were drawn at 130 °C and the draw ratio was in the range 6–30.

Methods

The wide-angle X-ray diffraction method with Ni-filtered Cu K_α radiation was applied. The studies were carried out by means of a flat camera equipped with a temperature chamber and a sample holder permitting the sample to be kept under various mechanical constraints. The texture axis was perpendicular to the primary beam, which in turn was perpendicular to the surface of the photographic film.

X-ray diffraction patterns were registered during stepwise increase of the temperature. At each step, the temperature was held constant for the time required for the registration of the pattern. The samples were kept under various mechanical constraints. Two different types of mechanical constraints were applied: constant load and constant length. In the case of constant load two different loads were applied. The larger one ($F = F_2$) causes an elongation of the sample while the smaller one ($F = F_1$) allows the sample to shrink during melting. Some samples were also heated without any constraints ($F = 0$).

The measured intensity I_m of scattered radiation was corrected for two effects:

$$I = \frac{I_m}{k_t k_T} \quad , \tag{9}$$

where k_t is the correction coefficient related to the changes in sample thickness during heating under constant load, and k_T is the correction factor due to the changes in the amplitude of an atom's vibration with temperature (temperature factor). Both corrections were determined in relation to the state of a sample at room temperature before heating. Neglecting the changes in the linear absorption coefficient μ with temperature, the coefficient k_t was calculated from [21]

$$k_t = \frac{\exp(-\mu t_T \cdot \sec 2\theta) \cdot \{1 - \exp[-\mu t_T \cdot (1 - \sec 2\theta)]\}}{\exp(-\mu t_{20} \cdot \sec 2\theta) \cdot \{1 - \exp[-\mu t_{20} \cdot (1 - \sec 2\theta)]\}} \quad , \tag{10}$$

where θ is Bragg angle, and t_T and t_{20} are the sample thicknesses at the actual temperature T and at room temperature, before heating, respectively. μ was assumed to be 4.0 cm^{-1}. The factor k_T was calculated from

$$k_T = \exp[-(B - B_{20}) \cdot \sin^2\theta/\lambda^2] \tag{11}$$

in which

$$B = 8\pi^2 \bar{u}^2 \tag{11a}$$

$$B_{20} = 8\pi^2 \bar{u}_{20}^2 \quad , \tag{11b}$$

where λ is the wavelength of radiation, and $\bar{u}^2$ and $\bar{u}_{20}^2$ are the mean-square displacements of atoms from their average positions measured in the direction perpendicular to the reflecting plane determined at actual and room temperature, respectively. The values of B and B_{20} were determined by linear extrapolation of the dependence of B on temperature found experimentally for polyethylene Marlex 6015 by Kilian [22]. The linearity of the $B(T)$ function is predicted theoretically [23] and is supported by several experimental results [23, 24].

The 110 and 200 reflections of the orthorhombic phase were analysed. The radial intensity distributions, $I_\beta(\theta)$, for different azimuthal angles β were first approximated by the sum of three Pearson VII functions of the form

$$I_\beta(\theta) = \frac{I_0}{\left[1 + 4\left(\frac{\theta - \theta_0}{H}\right)^2 \left(2^{1/m} - 1\right)\right]^m} \quad , \tag{12}$$

where I_0 and θ_0 are the intensity and the position of the maximum, respectively, H is the half width, m is a shape parameter determined for the 110 and 200 peaks, and for amorphous halo. The approximation was performed by means of a program for nonlinear optimization based on a Hook–Jeeves algorithm [25]. Since we did not find any essential changes in radial half width of either reflection as a function of azimuthal angle β, the orientation distributions of the crystallographic-plane normals 110 and 200 were determined from the dependence of I_0 for the 110 and 200 peaks upon the azimuthal angle β, further expressed as a function of the orientation angle α, determined by means of the Polany'i equation [26]:

$$\cos\alpha = \cos\theta_{hkl} \cdot \cos\beta \tag{13}$$

(note that the orientation angle α used by us is the orientation angle ϑ in Ziabicki's model). For each reflection, hkl, the function $I_0(\alpha)$ was approximated by the following sum of exponential functions:

$$I_0(\alpha) = I_1 \exp[A_1^2 \sin^2(\alpha - \alpha_{0,1})] + I_2 \exp[A_2^2 \sin^2(\alpha - \alpha_{0,2})] \quad . \tag{14}$$

In a previous paper [27] it was shown that Eq. (14) describes well the orientation distributions of the (hkl) planes in the gel-drawn UHMW PE samples investigated. The crystallite orientation distribution appeared to be a superposition of two functions representing broad and narrow contributions. The unknown parameters I, A, and α_0 have well-defined physical meanings. I is the maximum of the intensity occurring at the angle α_0 and A is related to the half width of the distribution. The subscripts 1 and 2 refer to the narrow and broad components of the crystallite orientation distribution. Each component of the sum (Eq. 14) has a clear physical meaning, representing the solution of a problem of the orientation distribution in a suspension of a rigid ellipsoids flowing in an elongational field. This function equally describes the orientation of dipoles in potential fields (e.g. electric or magnetic fields). The fraction u_n of the nth component, is expressed using the parameters I_n and A_n resulting from the approximation

$$u_1 = \frac{C_1}{(C_1 + C_2)} \tag{15}$$

$$u_2 = 1 - u_1 \quad , \tag{16}$$

where

$$C_n = \int_0^{\pi/2} I_n \exp[A_n^2 \sin^2(\alpha - \alpha_{0,n})] \sin\alpha \, d\alpha \quad , \tag{17}$$

where $n = 1, 2$.

The changes in crystallite orientation during heating were determined separately for each component of the orientation

distribution. For each crystallographic plane, (hkl) the orientation factor, $f_{hkl,n}$, was determined for the nth component from the equation

$$f_{hkl,n} = \frac{3\langle\cos^2\alpha\rangle - 1}{2} \quad , \tag{18}$$

where

$$\langle\cos^2\alpha\rangle = \frac{\int_0^{\pi/2} I_n \exp[-A_n^2 \sin^2(\alpha - \alpha_{0,n})] \cos^2\alpha \sin\alpha \, d\alpha}{\int_0^{\pi/2} I_n \exp[-A_n^2 \sin^2(\alpha - \alpha_{0,n})] \sin\alpha \, d\alpha} \quad . \tag{19}$$

The orientation function $f_{c,n}$ of the c-axis was then calculated according to the method proposed by Wilchinsky [28]. For the orthorhombic system of PE, considering the uniaxial symmetry of the system, it is possible to determine the orientation function of the c-axis from the measured values for two (hkl) crystallographic planes. In the case of the (1 1 0) and (2 0 0) planes the equation for determination of the orientation function of the c-axis has the following form [29]

$$f_{c,n} = -1.443845 \cdot f_{110,n} - 0.556155 \cdot f_{200,n} \quad . \tag{20}$$

The progress of melting was estimated by determination of the "local" crystallinity X related to the particular (hkl) plane of the nth component of the orientation distribution from the equation

$$X_n = \frac{\int_0^{\pi/2} \{I_n \exp[A_n^2 \sin^2(\alpha - \alpha_{0,n})]\}_{T_i} \cdot \sin\alpha \, d\alpha}{\int_0^{\pi/2} \{I_n \exp[A_n^2 \sin^2(\alpha - \alpha_{0,n})]\}_{T_{20}} \cdot \sin\alpha \, d\alpha} \quad , \tag{21}$$

where the integrals with subscripts T_i and T_{20} are proportional to the number of planes forming a particular reflection, hkl, at the actual temperature T_i, and at room temperature (before heating), respectively.

Moreover, phases formed as a result of the melting of orthorhombic crystallites were determined. The relative content κ of these phases was determined from

$$\kappa = \frac{\int_0^{\pi/2} I_0(\alpha) \sin\alpha \, d\alpha}{\int_0^{\pi/2} I_{0,\max}(\alpha) \sin\alpha \, d\alpha} \quad , \tag{22}$$

where $I_0(\alpha)$ denotes the intensities scattered in the phases at a given temperature, while $I_{0,max}(\alpha)$ denotes the corresponding intensities at the temperature at which the intensity reached a maximum.

The average statistical error of the arithmetic mean value of f_c estimated by repeating some measurements several times (usually 3) was found to be 0.001. The measured values of f_c are also loaded with some systematic error, mostly caused by the narrow linear range of the photographic emulsion as well as by neglecting instrumental broadening of the azimuthal profile. In order to ensure that systematic error is small and practically the same for all exposures, relatively low exposure times were used, and effort was made to keep similar exposure levels for all samples. The error caused by neglecting the instrumental broadening of the azimuthal profile is very low, because of good pinhole collimation. The reasons mentioned mean that the numerical values of the orientation factors determined in this work are more relative than absolute, but the relation between them is not affected by systematic error.

The maximum deviation of temperature during X-ray registration was $\pm 0.2°$.

Results

The structure before heating

X-ray diffraction patterns from the samples with various draw ratios registered at room temperature before heating are shown in Fig. 3. As reported previously [20, 29] the azimuthal profiles of the reflections registered are composed of two components with distributions differing in width. This indicates that there are two fractions of crystallites with different widths of the orientation distribution: very narrow (highly oriented crystallites, HOCs) and broad (low-oriented crystallites, LOCs). The approximation of the intensity distribution for the sample with the draw ratio $R = 6$ is shown in Fig. 4. It is seen from Fig. 4 that this approximation with Eq. (14) yields two nonzero values for the fraction of both components. An increase in the deformation leads to the reduction of the LOC fraction. Consequently, above some values of draw ratio, only the narrow component is visible (cf. Fig. 3c). The dependencies of the fractions, u_n, and the orientation factors, f_n, upon the draw ratio for both components of the orientation distribution were reported in Ref. [20].

The changes in crystallinity during heating

The changes in LOC and HOC content as a function of temperature are shown in Figs. 5 and 6. No differences between melting determined for the (1 1 0) and (2 0 0) planes were observed.

It is seen in Fig. 5 that the LOC content decreases with temperature. Comparison of Fig. 5a and b indicates that the complete disappearance of LOCs is reached at higher temperatures for the more deformed samples (temperature range between 142 and 145 °C, depending on the constraints) than for the low-deformed samples (temperature range between 135 and 138 °C, depending on the constraints). Moreover it is seen in Fig. 5 that the disappearance of LOCs occurs earliest for the most stressed samples (constant load F_2).

In the case of the HOC fraction (Fig. 6) there is also a temperature range in which an increase in the HOC fraction in some samples is observed during heating. This increase is the highest for slightly deformed samples (Fig. 6a), i.e. for the samples with large contributions of LOCs. In the case of highly deformed samples (Fig. 6c), containing only HOCs, heating over the whole temperature range causes exclusively a decrease in the HOC fraction. Comparison of Figs. 5 and 6 indicates, moreover, that the increase in the HOC fraction is always accompanied by a decrease in the LOC content. The facts presented indicate that an increase in the content of HOCs results in the transformation of LOCs. The question arises of whether the

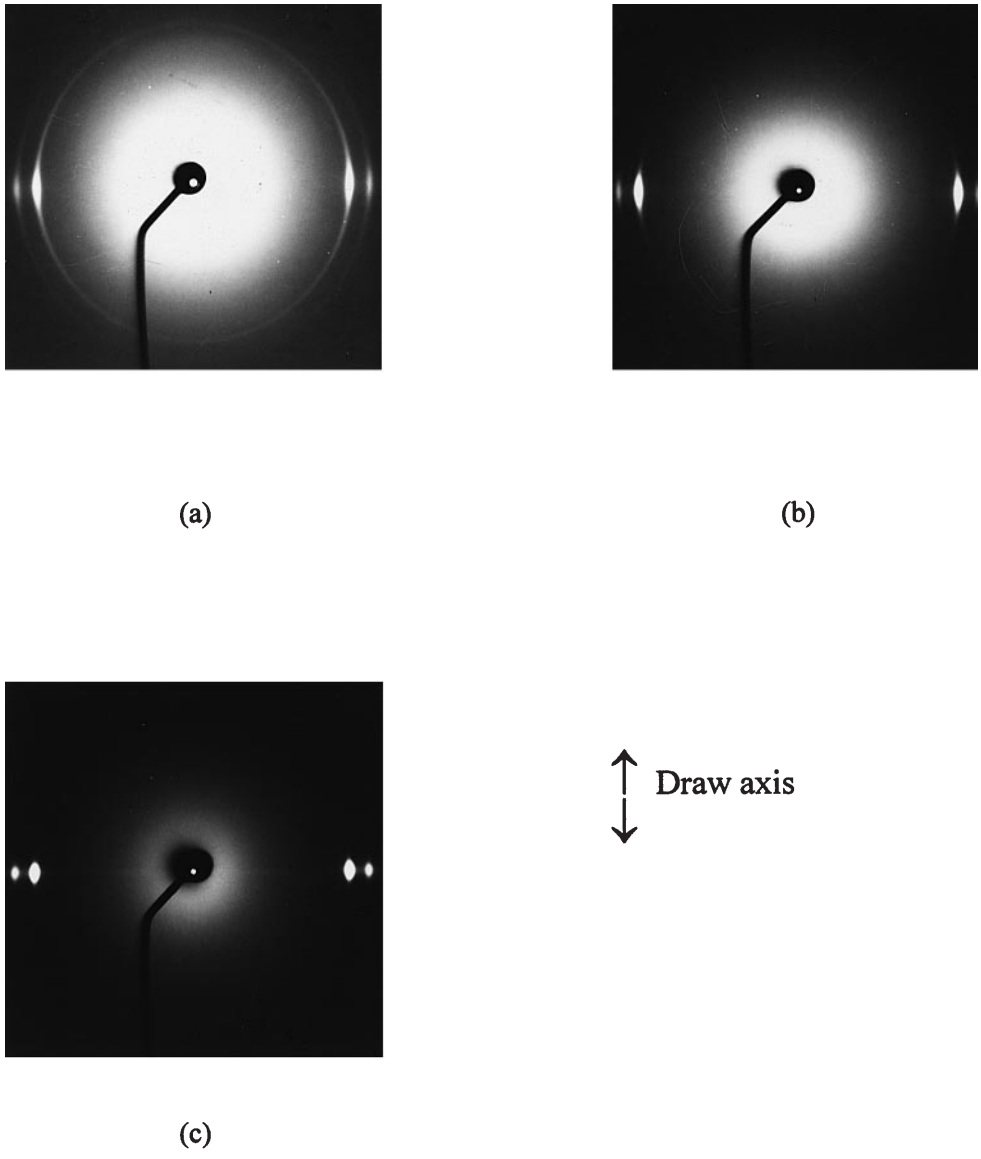

Fig. 3a–c X-ray diffraction patterns obtained from samples drawn to various draw ratios R. **a** $R = 6$, **b** $R = 14$ and **c** $R = 30$

LOCs undergo first melting and then recrystallize in more favourable orientations or whether they simply reorient without melting. In addition, the complete melting of HOCs occurs at temperatures higher than the melting of LOCs.

Some differences in the nature of the orthorhombic crystallites forming each of the components of the orientation distributions are deduced from the analysis of the disordered phases appearing as a result of melting. The formation of the typical amorphous phase was achieved by one of two ways, depending on the initial structure as well as on the mechanical constrains applied to the sample. When the low-deformed samples with a large LOC content were heated without any external stress, the typical amorphous phase was formed directly from orthorhombic crystallites. On the other hand, highly drawn samples, containing only HOCs, during heating under stress transform completely into a hexagonal phase, which melts to an amorphous phase upon further heating. The presence of the hexagonal phase is indicated by an additional diffraction line at $2\theta = 20.46^\circ$, appearing at elevated temperature. X-ray diffraction photographs showing the subsequent stages of melting in the situation when the hexagonal phase has formed are presented in Fig. 7.

The coexistence of both ways of melting, i.e. direct melting of orthorhombic crystallites into an amorphous melt, and a crystal–crystal transition from the orthorhombic to the hexagonal phase, was observed during heating under stress of the samples containing both components of the orientation distributions. The changes in the relative contents of the amorphous and the

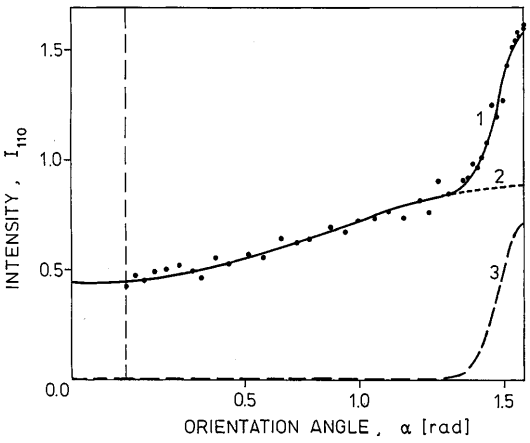

Fig. 4 Separation of the broad (*curve 2*) and narrow (*curve 3*) components of the azimuthal intensity distributions $I_o(\alpha)$ (*curve 1*) for the line 110 in the sample drawn to $R = 6$

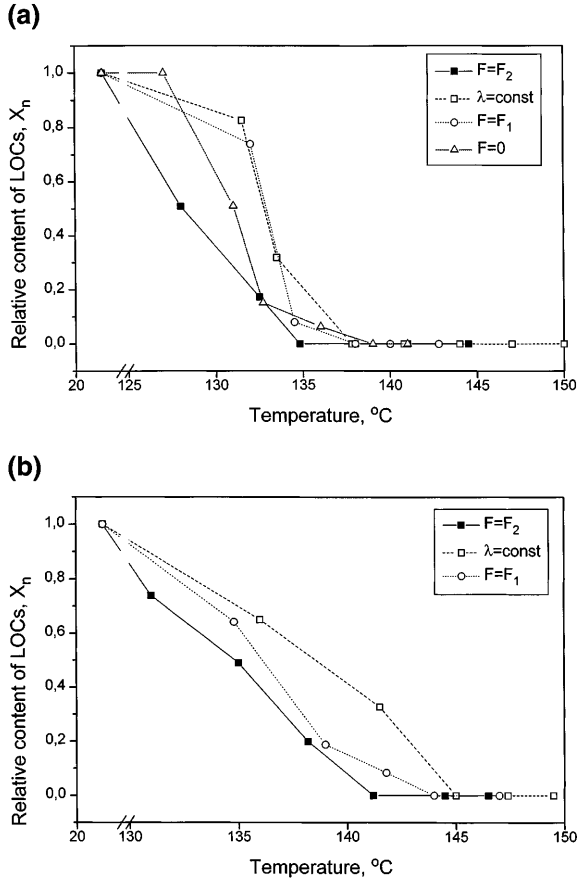

Fig. 5a, b Relative content, X_n, of low-oriented crystallites (*LOCs*) as a function of temperature at different mechanical constraints: $F = F_2$: high constant load causing the elongation of the sample; λ = constant length of the sample; $F = F_1$: low constant load allowing the sample to shrink; $F = 0$: no external constrains. **a** Samples with a draw ratio $R = 6$ and **b** samples with draw a ratio $R = 14$

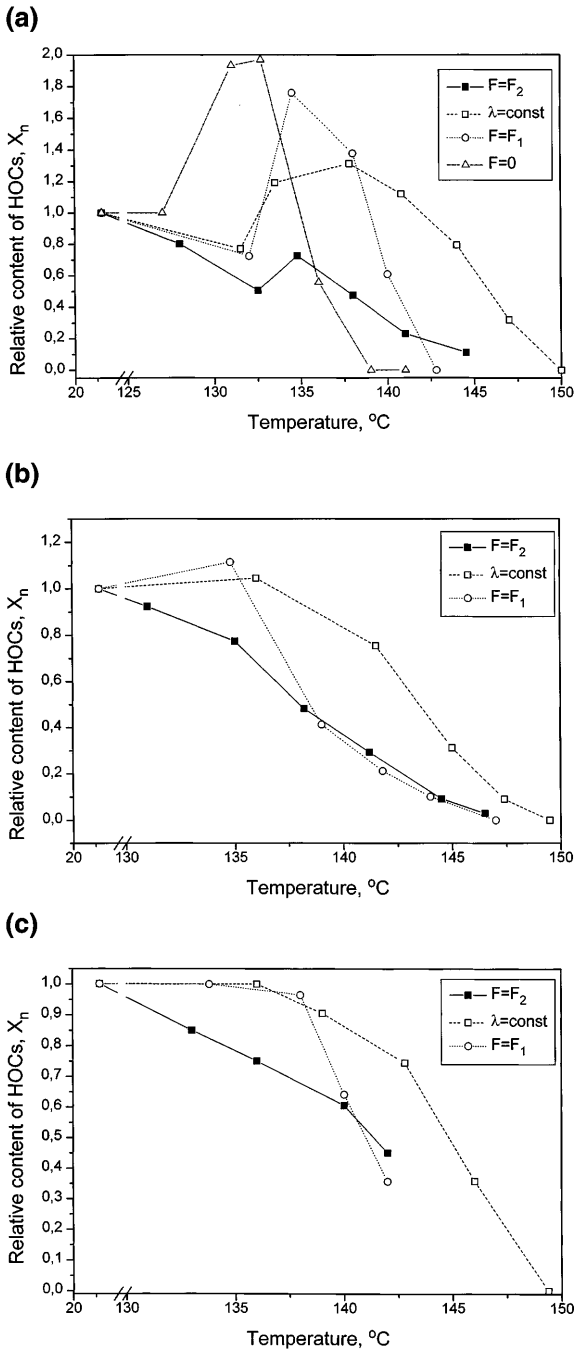

Fig. 6a–c Relative content, X_n, of highly oriented crystallites (*HOCs*) as a function of temperature at different mechanical constraints. **a** samples with a draw ratio $R = 6$, **b** samples with a draw ratio $R = 14$ and **c** samples with a draw ratio $R = 30$

hexagonal phases during heating of such a sample at constant length are shown in Fig. 8. At lower temperatures, a decrease in the LOC fraction is accompanied by an increase in the amorphous intensity and there is no evidence for the hexagonal phase. The increase in the

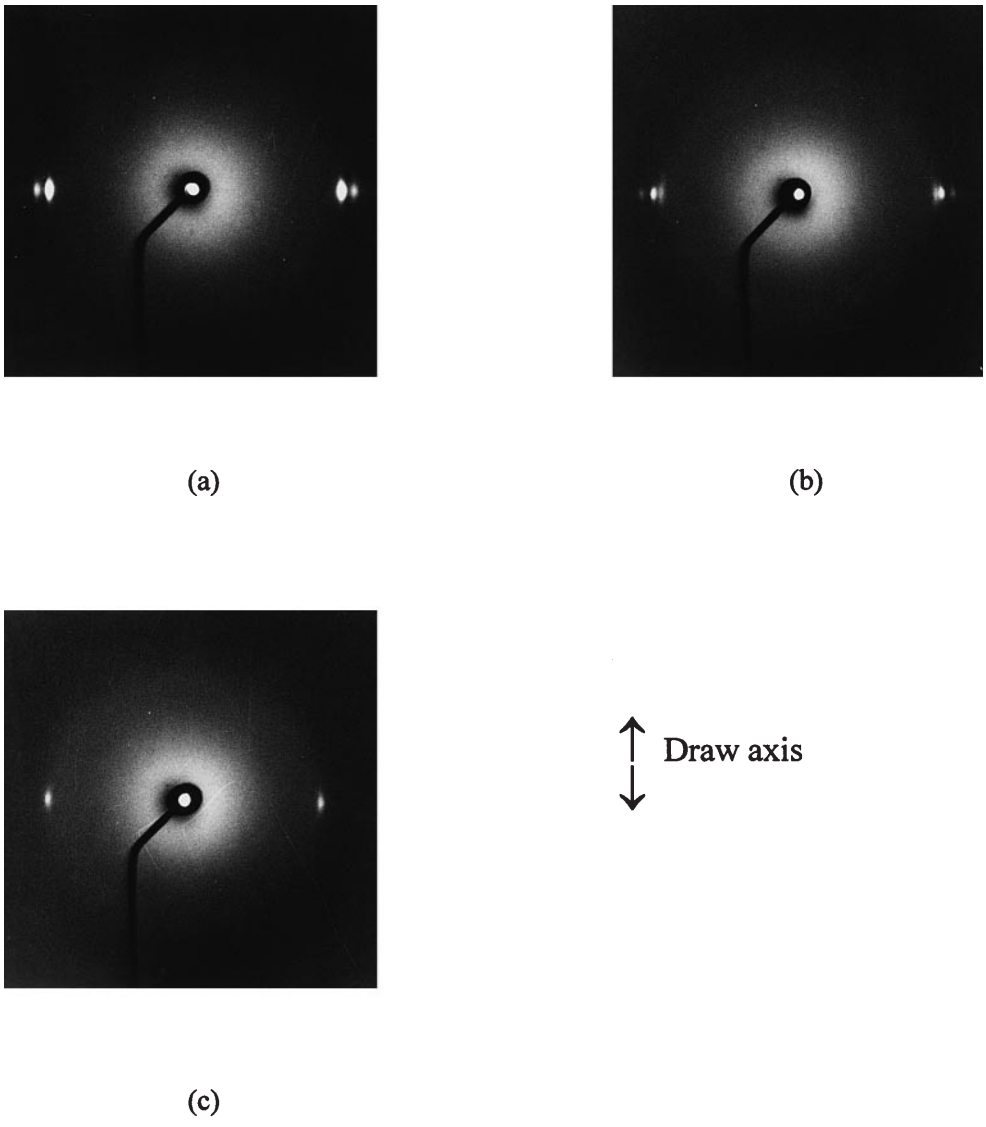

Fig. 7a–c X-ray diffraction photographs registered during subsequent stages of melting of the highly drawn sample kept under constant length. **a** $T = 20$ °C, the 1 1 0 and 2 0 0 lines of the orthorhombic phase, **b** $T = 147.4$ °C, the 1 1 0 and 2 0 0 lines of the orthorhombic phase and a line of the hexagonal phase, **c** $T = 149.5$ °C, the line of the hexagonal phase

amorphous intensity stops at the same temperature at which the LOCs completely disappear. Above this temperature, the content of the amorphous phase is constant, while the content of the hexagonal phase increases. The increase in the hexagonal phase intensity stops at the temperature of the complete disappearance of the HOC fraction. A further increase in the temperature causes a decrease in the content of hexagonal crystals, and again an increase in the amorphous phase content.

The changes in crystallite orientation during heating

Fraction of LOCs

In the case of low-deformed samples containing large fractions of LOCs (Fig. 9a) an increase in their degree of orientation during partial melting is observed in highly stressed samples which elongate under constant load and in those kept at constant length. In the later case the increase in the degree of orientation is weaker. When the sample is allowed to shrink during heating, the degree of orientation of the LOCs decreases during melting.

In the case of moderately deformed samples, containing only small fractions of LOCs (Fig. 9b) the tendency to increase their degree of orientation during melting is stronger. Even for the samples allowed to shrink slightly under constant load an increase in the degree of crystallite orientation during melting is observed.

Fraction of HOCs

The changes in orientation of HOCs during partial melting (Fig. 10, thick lines) depend on the mechanical

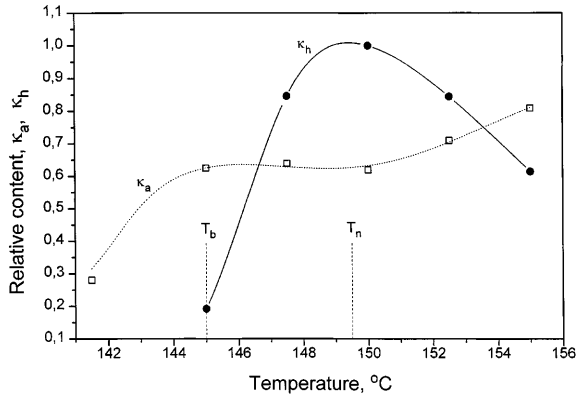

Fig. 8 Relative content of the amorphous κ_a, and hexagonal, κ_h, phase as a function of temperature. The temperature of the vanishing of the orthorhombic crystals constituting broad, T_b, and narrow, T_n, components of the orientation distribution are indicated

conditions. For the stressed samples, that elongate during heating as well as for those kept under constant length, a decrease in crystallinity is accompanied by an increase in their degree of orientation over the whole range of melting.

In the case of samples allowed to shrink under small load there is also some range of melting accompanied by an increase in the degree orientation of the HOCs. Such an increase was observed in the range of shrinkage below about 30% . Above about 30% shrinkage melting is always accompanied by a decrease in the degree of orientation of the HOCs. In the case of low-deformed samples (Fig. 10a) a decrease in the degree of orientation was observed at the beginning of melting even at low shrinkage.

In contrast to the behaviour observed during melting, the changes in the orientation of the HOCs in the range of increasing crystallinity (Fig. 10, thin lines) do not depend on the mechanical conditions. Regardless of the mechanical conditions an increase in the crystallinity of the HOC fraction is accompanied by a decrease in the degree orientation.

Discussion

The existence of two components in the orientation distribution, differing in width, indicates that there are two classes of molecules (crystallites) with different orientability. Some of the crystallites are oriented almost perfectly even at low-draw ratios (HOCs) while the others do not orient effectively during drawing (LOCs). The degree of orientation of LOCs increases with increasing deformation leading to the gradual vanishing of the fraction of LOCs. At draw ratio about 30 only the HOCs component remains. The deformation behaviour of semicrystalline polymers is usually discussed in terms of the deformation of a network with entanglements and

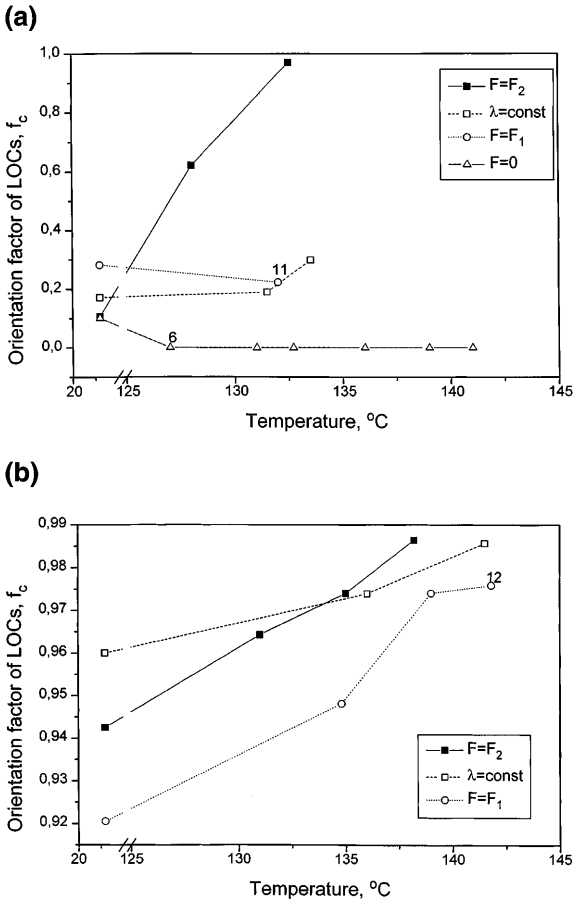

Fig. 9a, b Orientation function f_c for LOC component versus temperature. **a** $R = 6$ and **b** $R = 14$

crystallites acting as physical crosslinks [30]. In order to improve the drawability of UHMW PE the number of entanglements is reduced by crystallization from solution with low concentrated. On the other hand the minimum dilution limit necessary for the formation of a coherent gel is observed. This minimum value is related to the onset of coil overlap and therefore depends on the molecular weight of the polymer [31]. In our opinion there are two possible origins for the existence in our samples of two groups of molecules (crystallites) with different orientability. The first is related to the fact that in our solutions the polymer concentration exceeded only slightly the minimum value necessary for the formation of a coherent gel; therefore, it is expected that some of the molecules are not connected with others and do not transmit the applied force effectively. As a consequence they do not orient effectively during drawing. The second possibility is related to the temperature of drawing. Lemstra et al. [32] observed that two components with crystallite orientation distributions differing in width were formed during drawing of UHMW PE above the melting point of orthorhombic

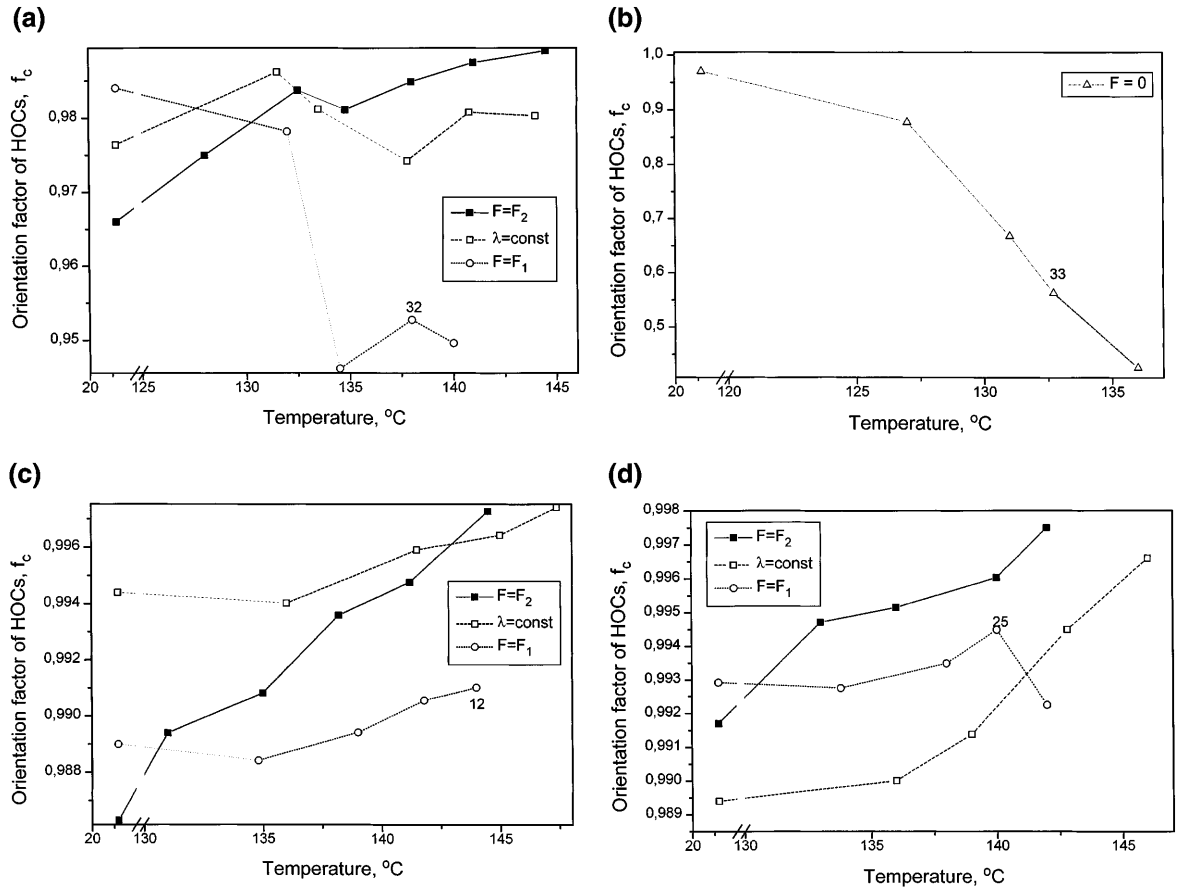

Fig. 10a–c Orientation function f_c for HOC component versus temperature. **a** $R = 6$, **b** $R = 14$ and **c** $R = 30$. *Thinner lines* indicate the ranges of increasing HOC content. The *numbers* indicate the actual shrinkage

crystallites (135 °C). They suggest [32] that during drawing in the melt, strain-induced crystallization occurs involving the high- molecular-weight part of the material whereas the lower-molecular-weight part of the sample relaxes during drawing. Although in our case the drawing temperature was slightly lower (130 °C) similar behaviour during drawing could be expected. Crystallites with broad orientation distributions would be formed during cooling by relatively short molecules in the relaxed state. A narrow orientation distribution would be formed during strain-induced crystallization from the high-molecular-weight part of the polymer. The final discrimination between the two possible origins of the coexistence of crystallites with different orientability needs direct investigations of the effect of the polymer concentration in solution and the temperature of drawing on the orientation distribution of crystallites.

The supposition that the molecules constituting LOCs are in a relaxed state, whereas those forming HOCs are long and taut is supported by the results of the investigations of phases formed during melting of orthorhombic crystallites. Orthorhombic LOCs melt directly to the typical amorphous phase while melting of HOCs under stress occurs through the intermediate hexagonal phase, which transforms into the amorphous phase upon further heating. The appearance of the hexagonal phase was reported by several authors during the melting of PE under stress or elevated pressure [32–40]. Their results indicate that the defective hexagonal phase (sometimes called pseudohexagonal) is formed as an intermediate state by the molecules which are strongly hampered during melting from adopting random coil conformations. It is expected that in the case of UHMW PE strong barriers against coiling appear when the molecules are entangled and especially when the molecules between entanglements are fully extended. Basset et al. [36] as well as Yasuniwa and Takemura [40] showed that under elevated pressure the hexagonal crystals of PE transform during crystallization directly into orthorhombic extended chain crystallites. Our previous results [20] dealing with the deformation of UHMW PE also indicate that the orthorhombic crystallites within the narrow distribution of orientation, which transform during melting to the hexagonal phase, are formed from extended chains, while the crystallites of the broad component of the orientation distribution are folded-chain crystallites. The concept of structure

inhomogenity in ultra-high-modulus PE fibres is widely accepted, being strongly supported by experimental results [41, 42]. According to the results of structural investigations extended chain fibrils are embedded in a semicrystalline matrix formed by lamellar crystallites. Fisher et al. [42] applied the idea of two components with different orientations to the analysis of wide-angle X-ray scattering orientation profiles of ultra-high-modulus PE and correlated this structure with the mechanical properties of the oriented polymer.

The fact that the HOCs formed by taut molecules melt at higher temperatures is justifiable in the light of the interpretation presented. Taut molecules are strongly hampered from adopting random coil conformations. This reduces the entropy of melting, and hence causes an increase in the melting temperature. On the other hand, we do not have any explanation for the increase in the content of HOCs observed at temperatures at which a simultaneous decrease in the LOC fraction occurs. Our results do not provide the answer to the question of whether this increase in crystallinity for HOCs is due to the reorientation of LOCs or whether it occurs as a result of recrystallization of melted LOCs. An increase in the amorphous halo intensity during the decrease in the LOC content indicates that at least some of the LOCs melt to the amorphous phase. On the other hand, the fast disappearance of LOCs at the highest stress indicates that the increase in the degree of orientation due to reorientation should be accounted for. It might be possible that during melting some of the LOCs become entangled and taut, which leads under high stress to recrystallization in the form of highly oriented aggregates.

The discussion of changes in crystallite orientation during melting needs an estimation of the stress acting in the system. Under all conditions applied the stress changes during heating so the effect of reorientation by the hydrodynamic field should be considered. We will start the discussion from the condition of constant length of a sample. In the case of a network with permanent crosslinks held at constant length, an increase in temperature should be accompanied by an increase in the stress. This increase is not only due to the change in entropic forces with temperature as is known from the theory of elasticity but is also due to changes in crystallinity shown by Flory [43]. In the case of a semipermanent physical network, such as gel-drawn UHMW PE, the situation is different. Since a great number of the crosslinks in UHMW PE crystallized from a solution are formed by crystallites, melting reduces the crosslinking density and hence the number of molecules transmitting the force. This is a strong factor acting towards a decrease in stress during melting of such semipermanent networks. Smook and Pennings [34] measured the retractive force during heating at constant length of oriented UHMW PE with $M_w = 4 \times 10^6$. They showed that the stress first increases with temperature approaching the maximum at about 125 °C. The beginning of the subsequent decrease in the stress coincides with the onset of the melting effect registered by differential scanning calorimetry on constrained samples.

Assuming the description of stress changes given in Ref. [34] to be also valid in our case we would expect the melting of our samples at constant length to be accompanied by a decrease in stress. Our results indicate that the melting in such conditions causes an increase in the degree of orientation of the remaining unmelted crystallites. This indicates that there is some mechanism for an increase in the degree of crystallite orientation during melting which predominates over the relaxation phenomena. This might be the kinetic factor introduced by Ziabicki [1, 2]. According to Ziabicki's model [1, 2] melting should start with the crystallites oriented perpendicular to the fibre axis, leading to an increase in the degree of orientation of the remaining unmelted crystallites.

t is expected that for samples allowed to shrink during heating the stress is lower in comparison with the constant length condition. The lower stress should make the relaxation of orientation easier. In our opinion an increase in the degree of orientation of crystallites formed from taut molecules registered below some shrinkage (about 30%) is strong evidence for the existence of a kinetic factor [1, 2] which is not compensated by relaxation. In sample shrinking above 30% , crystallinity is low which favours stress reduction and the relaxation of the orientation of crystallites formed by taut molecules. The relaxation of crystallite orientation also prevails during the melting of crystallites formed by relaxed molecules in the low-deformed samples allowed to shrink under constant load. The fact that in the case of highly deformed material the orientation of crystallites formed by relaxed molecules increases even for slightly shrinking samples is not completely clear.

It is expected that in the case of samples which elongate during heating under constant load the stress is higher in comparison with those kept under constant length. The observed increase in the degree of crystallite orientation during melting of both types of crystallites in the elongating samples is, at least to some extent, due to hydrodynamic reorientation.

Our results also show that in the range of increasing content of HOCs their orientation decreases independently of external constraints. The discussion of this point needs further investigations of the mechanism of the observed increase in crystallinity.

Acknowledgement We would like to express our sincere thanks to A. Ziabicki for helpful discussion and valuable comments regarding his model of crystal nucleation in oriented systems. This work have been supported in part by Research Grant 7 T08E 027 10 offered by the Polish Committee of Scientific Research (Komitet Badań Naukowych).

References

1. Ziabicki A (1977) J Chem Phys 66: 1638
2. Ziabicki A (1986) J Chem Phys 85: 3042
3. Ziabicki A, Jarecki L (1994) J Chem Phys 101: 2267
4. Ziabicki A, Jarecki L (1978) Colloid Polym Sci 256: 332
5. Krigbaum WR, Roe RJ (1964) J Polym Sci Part A 2: 4931
6. Ziabicki A (1996) Colloid Polym Sci 274: 705
7. Illers K-H (1970) Angew Makromol Chem 12: 89
8. Cousin P, Michel M (1987) Preprints of the European Symposium on Polymeric Materials, Lyon, France, September 14–18, GPCO4
9. Krigbaum WR, Maruno S (1968) J Polym Sci Polym Phys Ed 6: 1733
10. Wasiak A (1981) Coll Polym Sci 259: 135
11. Cesari M, Perego G, Zazetta A, Gargani L (1980) Makromol Chem 180: 1143
12. Hashimoto T, Saijo K, Kość M, Kawai H, Wasiak A, Ziabicki A (1985) Macromolecules 18: 472
13. Murase S, Kakamoto K, Kudo K (1996) Sen'i Gakkaishi 52: 450
14. (a) Ziabicki A, Jarecki L (1985) In: Ziabicki A, Kawai H (eds) High-speed fiber spinning. Wiley Interscience, New York, pp 225; (b) Perez G In: Ziabicki A, Kawai H (eds) High-speed fiber spinning. Wiley Interscience, New York, pp 333
15. Smith P, Lemstra PJ (1980) J Mater Sci 15:505
16. Smith P, Lemstra PJ, Pijpers JPL, Kiel AM (1981) Colloid Polym Sci 259: 1070
17. Smith P, Lemstra PJ, Kalb B, Pennings AJ (1979) Polym Bull 1: 733
18. Smith P, Lemstra PJ (1979) Makromol Chem 180: 2983
19. Sajkiewicz P (1991) Polimery 36: 245
20. Wasiak A, Sajkiewicz P (1993) J Mater Sci 28: 6409
21. Alexander LE (1969) X-ray diffraction methods in polymer science. Wiley, Chichester
22. Kilian HG (1962) Kolloid ZZ Polym 183: 1
23. Cruickhank DWJ (1956) Acta Crystallogr 9: 1005
24. Lonsdale K, El Sayed K (1965) Acta Crystallogr 19: 487
25. Bazaraa MS, Shetty CM (1979) Nonlinear programming theory and algorithms. Wiley, New York
26. Polanyi M (1921) Z Phys 7: 149
27. Sajkiewicz P, Wasiak A (1990) J Appl Crystallogr 23: 88
28. Wilchinsky Z (1959) J Appl Phys 30: 729
29. Sajkiewicz P (1989) Rep Inst Fund Technol Res 12: 3
30. Capaccio G, Gibson AG, Ward IM (1979) In: Cifferi A, Ward IM (eds) Ultra-high modulus polymers. Applied Science, London, pp 12–61
31. Smith P, Lemstra PJ, Booij HC (1981) J Polym Sci Polym Phys Ed 19:877
32. Lemstra PJ, van Aerle NAJM, Bastiaansen CWM (1987) Polym 19:85
33. Clough SB (1971) J Appl Polym Sci 15:2141
34. Smook J, Pennings AJ (1984) Colloid Polym Sci 262:712
35. Yasuniwa M, Enoshita R, Takemura T (1976) Jpn J Appl Phys 15:1421
36. Basset DC, Block S, Piermarini G (1974) J Appl Phys 45:4146
37. Ungar G, Keller A (1980) Polymer 21:1273
38. Pennings AJ, Zwijnenburg A (1979) J Polym Sci Polym Phys Ed 17:1011
39. Asahi T (1984) J Polym Sci Polym Phys Ed 22:175
40. Yasuniwa M, Takemura T (1974) Polymer 15:661
41. Gibson AG, Davis GR, Ward IM (1978) Polymer 19:688
42. Fisher L, Haschberger R, Ziegeldorf A, Ruland W (1982) Colloid Polym Sci 260:174
43. Flory PJ (1947) J Chem Phys 15:397